Functional morphology of the Triassic apex predator *Saurosuchus galilei* (Pseudosuchia: Loricata) and convergence with a post-Triassic theropod dinosaur

Fawcett, Molly J.; Lautenschlager, Stephan; Bestwick, Jordan; Butler, Richard J.

DOI:
10.1002/ar.25299

Received: 5 April 2023 | Revised: 11 July 2023 | Accepted: 13 July 2023

DOI: 10.1002/ar.25299

RESEARCH ARTICLE

The Anatomical Record WILEY

Functional morphology of the Triassic apex predator *Saurosuchus galilei* (Pseudosuchia: Loricata) and convergence with a post-Triassic theropod dinosaur

Molly J. Fawcett | **Stephan Lautenschlager** | **Jordan Bestwick** | **Richard J. Butler**

School of Geography, Earth and Environmental Sciences, University of Birmingham, Birmingham, UK

Correspondence
Stephan Lautenschlager and Jordan Bestwick, School of Geography, Earth and Environmental Sciences, University of Birmingham, Edgbaston, Birmingham B15 2TT, UK.
Email: S.lautenschlager@bham.ac.uk and jordan.bestwick92@gmail.com

Funding information
Leverhulme Trust, Grant/Award Number: RPG-2019-364

Abstract

Pseudosuchian archosaurs, reptiles more closely related to crocodylians than to birds, exhibited high morphological diversity during the Triassic and are thus associated with hypotheses of high ecological diversity during this time. One example involves basal loricatans which are non-crocodylomorph pseudosuchians traditionally known as "rauisuchians." Their large size (5–8+ m long) and morphological similarities to post-Triassic theropod dinosaurs, including dorsoventrally deep skulls and serrated dentitions, suggest basal loricatans were apex predators. However, this hypothesis does not consider functional behaviors that can influence more refined roles of predators in their environment, for example, degree of carcass utilization. Here, we apply finite element analysis to a juvenile but three-dimensionally well-preserved cranium of the basal loricatan *Saurosuchus galilei* to investigate its functional morphology and to compare with stress distributions from the theropod *Allosaurus fragilis* to assess degrees of functional convergence between Triassic and post-Triassic carnivores. We find similar stress distributions and magnitudes between the two study taxa under the same functional simulations, indicating that *Saurosuchus* had a somewhat strong skull and thus exhibited some degree of functional convergence with theropods. However, *Saurosuchus* also had a weak bite for an animal of its size (1015–1885 N) that is broadly equivalent to the bite force of modern gharials (*Gavialis gangeticus*). We infer that *Saurosuchus* potentially avoided tooth–bone interactions and consumed the softer parts of carcasses, unlike theropods and other basal loricatans. This deduced feeding mode for *Saurosuchus* increases the known functional diversity of basal loricatans and highlights functional differences between Triassic and post-Triassic apex predators.

KEYWORDS

Allosaurus, loricatan, predator, *Saurosuchus*, theropod, Triassic

1 | INTRODUCTION

Middle and Late Triassic pseudosuchian archosaurs—reptiles more closely related to crocodylians than to birds—exhibit higher levels of morphological disparity than at any other point in their evolutionary history (Brusatte et al., 2008, 2010; Nesbitt, 2011; Stubbs et al., 2013). Many of the skeletal bauplans exhibited by early pseudosuchians have been described as convergent with distantly related dinosaurs from the Jurassic and Cretaceous (Stocker et al., 2016). Examples include the gracile, bipedal stances and skulls with large orbits and edentulous jaws of shuvosaurid poposauroids, which are similar to those of ornithomimids (Bestwick et al., 2022; Nesbitt, 2007; Nesbitt & Norell, 2006), the robust limbs and armored bodies of aetosaurs which are similar to those of ankylosaurians (Desojo et al., 2013; Parker et al., 2021) and the elongate rostra and expanded neural spines of phytosaurs which are reminiscent of some spinosaurids (Stocker et al., 2016). Pseudosuchians thus likely filled a wide range of ecological roles and are regarded as the dominant tetrapod group in Middle and Late Triassic terrestrial food webs (Brusatte et al., 2008; Stocker et al., 2016).

Another well-known example of convergence involves a paraphyletic grade of non-crocodylomorph loricatans, traditionally referred to as "Rauisuchia" and are hereafter termed basal loricatans (*sensu* Nesbitt & Desojo, 2017). These pseudosuchians had a near-cosmopolitan distribution, although they are as-yet unknown from Antarctica and Australasia, and were among the largest terrestrial animals of the Middle and Late Triassic with some taxa estimated to have reached 8+ m in length (França et al., 2011; Nesbitt et al., 2013; Tolchard et al., 2021; Young, 1973). Basal loricatans share several morphological traits with theropod dinosaurs such as allosaurids and tyrannosaurids, including large dorsoventrally deep skulls, ziphodont dentitions (labio-lingually compressed in shape with serrated carinae; Brink et al., 2015) and even bipedality in a few taxa (e.g., *Postosuchus* spp.; Alcober, 2000; Brusatte et al., 2009; Chatterjee, 1985; Mujal et al., 2022; Weinbaum, 2011, 2013). These morphological similarities, along with their large size and being identified the perpetrators of bite marks on numerous fossil bones, implicate basal loricatans as the "apex predators" of Middle and Late Triassic food webs, performing the same ecological role as later evolving theropods (Alcober, 2000; Chatterjee, 1985; Gower, 2000; Klein et al., 2017; Mastrantonio et al., 2019; Mujal et al., 2022; Nesbitt et al., 2013; Roberto-Da-Silva et al., 2018; Weinbaum, 2011, 2013).

However, the ecological classification of apex predator is rather broad as it generally refers to the elevated trophic position of a taxon within a food web (Wallach et al., 2015). The term can even be argued as simplistic since it rarely considers the functional repertoires of predators, which can have subtly different impacts on the environments in which they live (DeVault et al., 2003; Wallach et al., 2015; Wilkenros et al., 2013). For example, in the African savannah lions (*Panthera leo*) and spotted hyenas (*Crocuta crocuta*) are both recognized as apex predators with overlapping prey preferences (Schubert et al., 2010; Sinclair et al., 2003; van Valkenburgh et al., 1990). However, hyenas are renowned for their more frequent processing and consumption of bones (i.e., osteophagy) and thus leave less food available for scavenging (DeSantis et al., 2013; Ogada et al., 2012; Schubert et al., 2010; van Valkenburgh et al., 1990). Similar inferences are possible for extinct taxa such as theropod dinosaurs (Sakamoto, 2010). Late Cretaceous tyrannosaurids, for example, are infamous for exhibiting higher degrees of osteophagy relative to other theropods based on extremely high predicted bite forces from biomechanical models, heavily worn teeth and bone-rich coprolites (Chin et al., 1998; Gignac & Erickson, 2017; Rayfield, 2004, 2005; Sakamoto, 2010; Schubert & Ungar, 2005; Snively & Russell, 2007; but see Winkler et al., 2022). Allosaurids, in contrast, had weaker bite forces than tyrannosaurids based on biomechanical models and instead are inferred as employing a "strike-and-tear" technique aided by strong ventroflexive cervical musculature to procure and consume prey with relatively fewer tooth–bone interactions (Montefeltro et al., 2020; Rayfield et al., 2001; Snively et al., 2013). The hypothesis that basal loricatans are direct Triassic functional analogues of theropods is therefore premature without quantitative investigation into the functional morphology of these pseudosuchians. Furthermore, qualitative assessments of function based on superficially similar forms can be misleading as demonstrated for different herbivorous, phylogenetically disparate, but functionally convergent dinosaurs (Lautenschlager et al., 2016).

One basal loricatan suitable for study is the quadrupedal *Saurosuchus galilei* from the Ischigualasto Formation (Carnian to early Norian ~231.4–225.9 Ma) of Argentina (Martínez et al., 2013; Walker et al., 2013). At an estimated 7 m total length, *Saurosuchus* is one of the largest basal loricatans known and is similar in size to several groups of Jurassic and Cretaceous theropods (Alcober, 2000; Nesbitt et al., 2013; Sill, 1974; Trotteyn et al., 2011). In particular, an almost completely preserved *Saurosuchus* cranium (División de Paleontología de Vertebrados del Museo de Ciencias Naturales y Universidad Nacional de San Juan, San Juan, Argentina [PVSJ] 32; a partial but poorly preserved mandible is also present) is similar in size to an *Allosaurus fragilis*

cranium, and has good three-dimensional preservation including the posterior braincase (although some deformation and erosion are still present; Alcober, 2000). Remarkably, despite its large size the specimen represents a late-stage juvenile and thus had not yet attained its final size (Alcober, 2000). *Saurosuchus* is therefore a suitable case study for investigating the functional behaviors of basal loricatans and their potential similarity to theropods.

Here, we restore the original morphology of the *Saurosuchus* cranium and perform the first biomechanical study of a basal loricatan to investigate its functional morphology. We include a previously published 3D model from the theropod *Allosaurus fragilis* (Lautenschlager, 2015; Montefeltro et al., 2020; Rayfield, 2005; Rayfield et al., 2001) as our functional analogue to assess the degree of functional convergence between basal loricatans and post-Triassic theropod dinosaurs.

2 | MATERIALS AND METHODS

2.1 | Specimen information

We obtained our data for *Saurosuchus galilei* from the public repository of computed tomography (CT) scan data Digimorph (http://www.digimorph.org/specimens/Saurosuchus_galilei/) provided by and courtesy of Dr Matthew Colbert and Dr Jessie Maisano. The specimen (PVSJ 32) was originally CT scanned at the University of Texas High-Resolution x-ray CT Facility. Scan settings include 420 kV (energy), 4.7 mA (current), 2 brass filters, an air wedge, a translate-rotate scan, an integration time of 16 ms, a slice thickness of 2.0 mm, 661 mm S.O.D., 2 views, 1 ray per view, 2 samples per view, interslice spacing of 1.8 mm, 400 mm field of reconstruction, a reconstruction offset of 500, and a reconstruction scale of 150. Slices were in eight-bit mode. Scans were mirrored (i.e., right and left lateral sides are the opposite of the fossil specimen), but this has been corrected during the retrodeformation and reconstruction process.

The partially preserved PVSJ 32 mandible is represented only by the anterior portions of the dentary, splenial, and coronoid (Alcober, 2000) and a box-modeling approach (Rahman & Lautenchlager, 2016) was employed to create a complete (but somewhat hypothetical) mandible to be used as a reference for the muscle reconstruction. Rather than creating a completely new lower jaw, the mandible of *Allosaurus fragilis* (Museum of the Rockies, Bozeman, Montana [MOR] 693, see Rayfield et al., 2001; for scanning details) was modified to complete the *Saurosuchus* skull model. *Allosaurus* was chosen as the initial template for the hypothetical mandible because most Triassic theropod and basal loricatan mandibles are also poorly preserved (e.g., Garcia et al., 2021; Weinbaum, 2011). *Allosaurus* mandibles, in contrast, are preserved in great detail with high-quality three-dimensional scans available (Rayfield et al., 2001). Furthermore, fragments of preserved *Saurosuchus* mandibles show several features that are superficially more similar to theropods like *Allosaurus*, such as an anterior process of the coronoid, than to more closely related basal loricatans (Alcober, 2000; Sill, 1974). Similar to *Allosaurus*, the mandible of *Saurosuchus* was likely medially curved due to the ventrolaterally projecting pterygoid flanges constraining the medial extent of the posterior dentary and surangular region. To guide model generation of the lower jaw, we followed the reconstruction in Alcober (2000) and adjusted the model to match the published figure. Our hypothetical *Saurosuchus* mandible undoubtedly brings a minor element of uncertainty to the biomechanical feeding simulations of the skull as the hypothesized mandibular muscle attachment sites represent a generic archosaurian anatomy rather than the "true" *Saurosuchus* or basal loricatan anatomy. For this reason, we restricted the biomechanical simulations to the cranium and used the lower jaw as a reference for muscle reconstructions only. However, this still enables the identification of more and less likely functional behaviors to constrain the functional repertoire of *Saurosuchus*. Our cautious yet informed experimental approach therefore allows us to draw informed interpretations on the functional morphology of this pseudosuchian and to make comparisons with theropods.

We also modeled the complete MOR 693 *Allosaurus fragilis* skull as the comparative theropod analogue due to its similar cranial size to PVSJ 32 (610 and 720 mm, respectively along an anterior–posterior axis) and availability of high-quality, three-dimensional scans.

2.2 | Retrodeformation and digital reconstruction

The *Saurosuchus* CT image files were imported into AVIZO Lite (Version 9.3.0, Visualisation Science Group) for segmentation. The individual cranial elements were highlighted and separately labeled using the AVIZO segmentation editor to produce surface models and volumes using a combination of automatic thresholding (where resolution permitted) and manual tracing of elements. All elements were subsequently imported into Blender 2.80 (Blender.org) and then retrodeformed to their hypothesized original morphology and realigned to restore the cranium to an approximate nondeformed condition (Figure 1). The restoration process followed the steps of Lautenschlager (2016) and was informed by: the topographic relationships

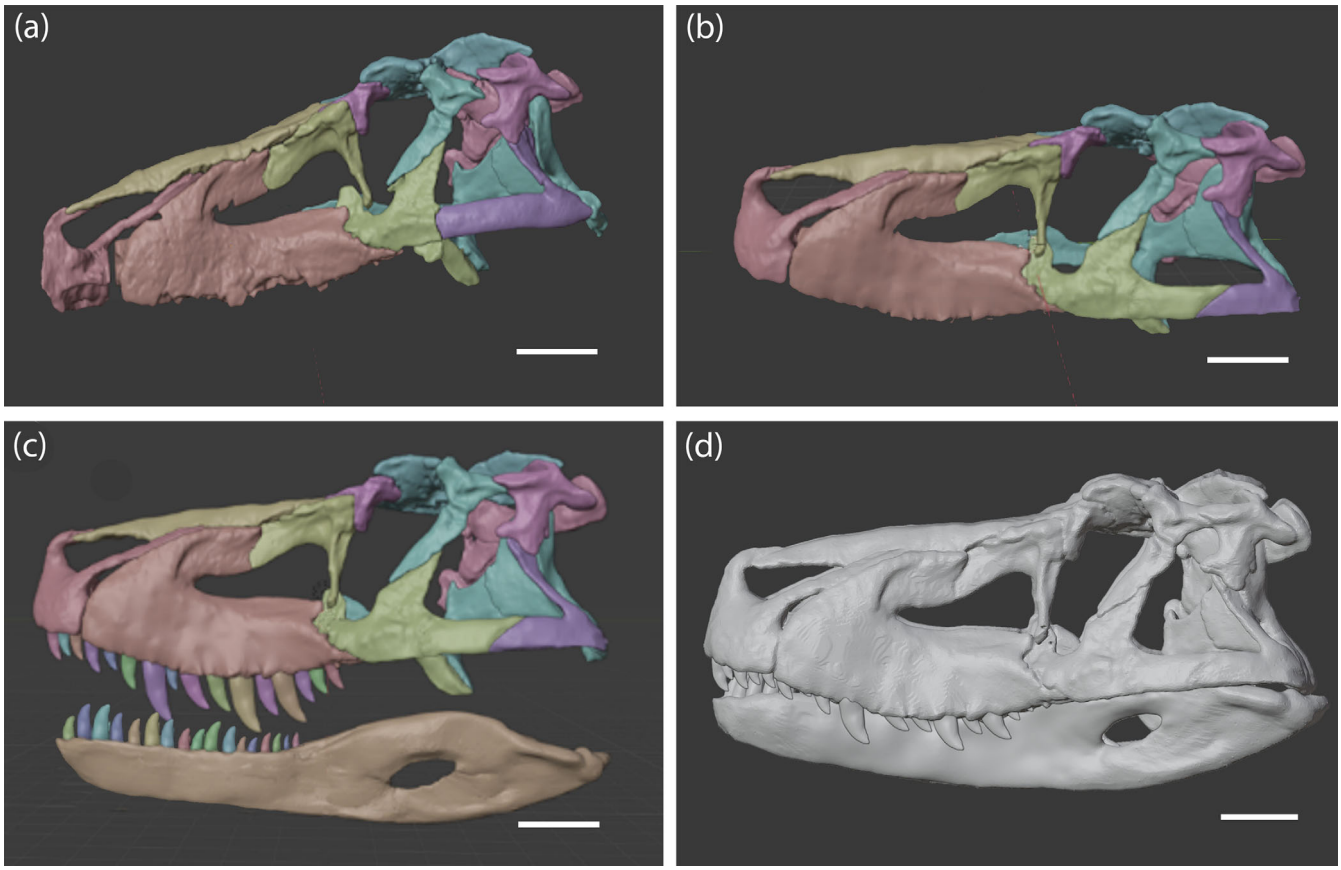

FIGURE 1 Reconstructed cranial anatomy of *Saurosuchus galilei* (PVSJ 32). (a) Digital model of the segmented specimen, (b) cranium with realigned elements and postmortem degradation features, such as cracks and holes, corrected, (c) cranium and hypothetical mandible based on an adjusted *Allosaurus fragilis* mandible, both with box-modeled archosaur teeth inserted into alveoli, and (d) fully restored morphology used for finite element models in this study. Note the subnarial fenestra just ventral to the naris is indicative of the juvenile condition of the specimen. Scale bar 10 cm.

of individual elements in the 3D CT scan data; identification and subsequent repair of cracks and holes; and osteological comparisons with closely related loricatans (e.g., *Batrachotomus kupferzellensis*, *Prestosuchus* spp.; Butler et al., 2022; Desojo et al., 2020; Roberto-Da-Silva et al., 2018). Considerable deformation had occurred on the right side of the cranium; thus, the left side was duplicated and mirrored for the reconstruction, assuming bilateral symmetry. An exception was the right premaxilla, which had suffered less deformation of the two bones and was thus duplicated and served as a mirrored substitute for the left premaxilla. PVSJ 32 represents a juvenile based on several features including subnarial fenestrae between the premaxillae and maxillae (Figure 1) and an open suture between the exoccipitals and basioccipitals (Alcober, 2000). These features were included in the fully restored model to increase the degree of model realism.

The hypothetical *Saurosuchus* mandible was created by importing the MOR 693 *Allosaurus* mandible into Blender and retrodeforming the model to a hypothesized morphology based on known *Saurosuchus* material (Alcober, 2000; Sill, 1974) and by comparisons with closely related loricatans where appropriate (Figure 1). Some of the main modifications include (but are not inclusive of all changes): (i) laterally widening the mandible, particularly for the posterior half, so that it articulates correctly with the quadratojugals (Alcober, 2000; Sill, 1974); (ii) near-removal of the pronounced ventral deflection along the posteroventral surfaces of the dentaries and splenials (Chure & Loewen, 2020) so that only minimal ventral deflection is observed between the border of the dentaries and angulars. Unlike in other loricatans, such as *Batrachotomus* and *Postosuchus*, the mandible of *Saurosuchus* lacks a dorsally or dorsoventrally expanded symphyseal region based on known preserved material (Alcober, 2000; Nesbitt et al., 2013). (iii) modifying the anterodorsal surface of the surangulars to be markedly convex in shape (Alcober, 2000; Mastrantonio et al., 2019). As the surangular region is not preserved, it is unclear whether *Saurosuchus* possessed an expanded surangular shelf (as in *Batrachotomus* and *Postosuchus*) which may

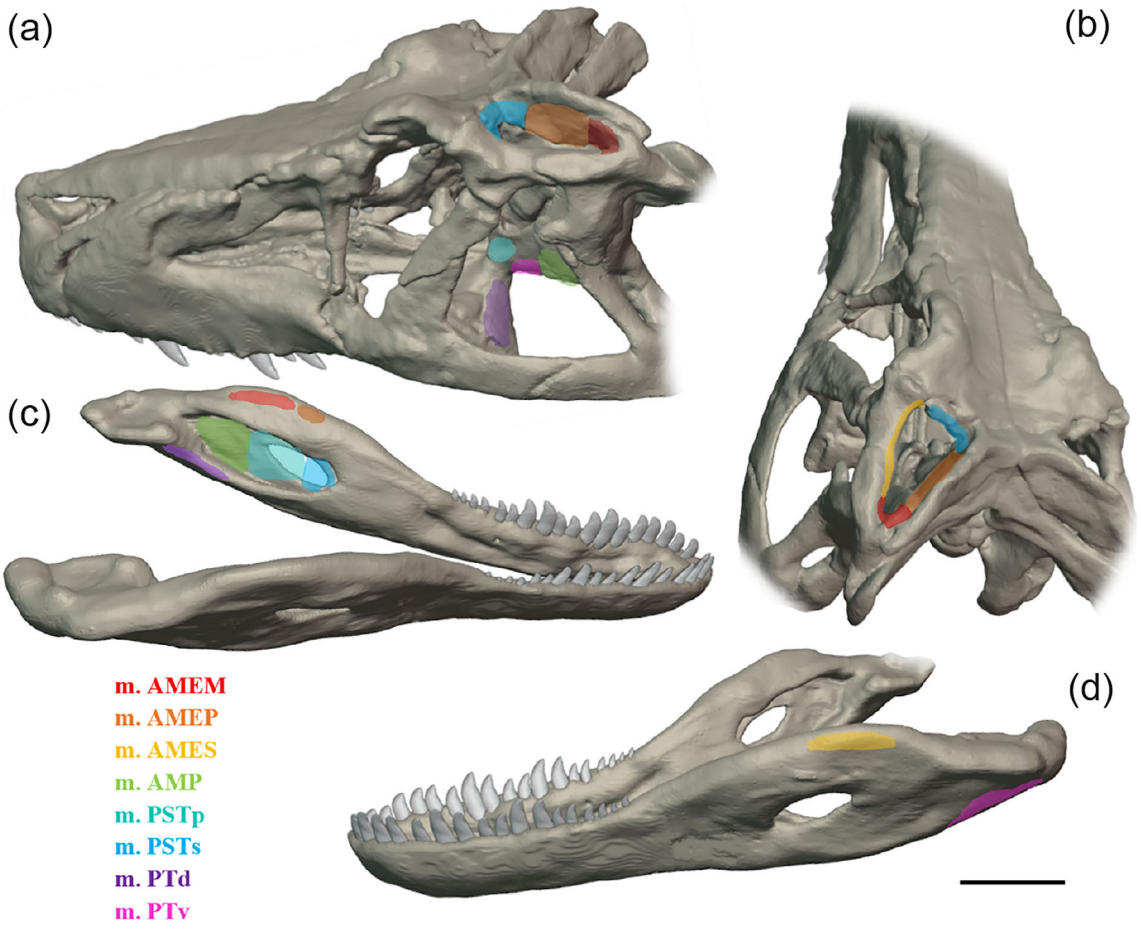

FIGURE 2 Muscle attachment locations of the retrodeformed *Saurosuchus galilei* cranium and the hypothetical mandible based on an adjusted *Allosaurus fragilis* mandible. (a) Left cranium surface in dorsaolateral view, (b) cranium in dorsal view with a slight lateral tilt, (c) right mandible surface in medial view, and (d) left mandible surface in lateral view. m. AMEM (red), m. adductor mandibulae externus medialis; m. AMEP (orange), m. adductor mandibulae externus profundus; m. AMES (yellow) m. adductor mandibulae superficialis; m. AMP (green), m. adductor mandibulae posterior; m. PSTp (turquoise), m. pseudotempralis profunuds; m. PSTs (blue), m. pseudotemporalis superficialis; m. PTd (purple), m. pterygoideus dorsalis; m. PTv (pink), m. pterygoideus ventralis. Note the hypothetical morphology of the adjusted mandible results in the mandibular muscle attachment sites representing a generic archosaur condition as opposed to the "true" *Saurosuchus* or basal loricatan condition. Scale bar 10 cm.

have influenced the muscle reconstruction slightly. However, *Saurosuchus* lacks the prominent shelf on the jugal region which may be a counterpart to and indicative of a surangular shelf. We have therefore opted for a more generic reconstruction of the surangular region. (iv) moving the mandibular fenestrae slightly posteriorly so when viewed laterally in articulation with the cranium, the fenestrae are level with the postorbital-jugal bar (Gower, 1999; Weinbaum, 2011). As the specimen does not preserve any teeth, a generic carnivorous archosaur tooth was box-modeled (see Rahman & Lautenchlager, 2016). The tooth was then duplicated and the size and position were adjusted with the alveoli morphology of PVSJ 32 and reconstructions of Alcober (2000) guiding the reconstruction of the complete tooth row.

2.3 | Muscle reconstructions

Muscle origination sites on the *Saurosuchus* cranium (Figure 2) were identified for each jaw adductor muscle independently based on osteological correlates such as muscle scars, ridges and depressions. Muscle insertion sites on the adjusted mandible (Figure 2) were based on the same criteria, assuming a largely similar jaw adductor arrangement across archosaurs following von Baczko (2018), Bestwick et al. (2022), and Holliday (2009). As a first step, the origin and insertion sites of each muscle were connected by individual point-to-point connections. This allowed the general muscle arrangement to be identified, as well as smaller edits of the attachment sites to avoid muscle intersections following the approach of Lautenschlager (2013). Then the full muscle bodies were

fleshed out in Blender using a combination of box modeling and the in-built sculpting tools.

2.4 | Bite force

The length and volume of each adductor muscle were obtained using the measurement in Blender and these values were subsequently used to calculate the physiological cross-sectional area (Table 1), under the assumption that fiber length is equal to muscle length (as in Gignac & Erickson, 2017). Muscle force was then calculated for each muscle individually (i.e., for one side of the cranium), by multiplying cross-sectional area by an isometric muscle stress value of 30 N cm^{-2} (Table 1). It should be noted that muscle force estimates calculated this way yields close to minimal forces (Bates & Falkingham, 2018; Cost et al., 2020).

2.5 | Finite element analysis

All 3D models were imported into Hypermesh 13 (Altair Engineering) for the generation of solid tetrahedral meshes (*Saurosuchus* cranium comprises ~3,741,217 elements). Both crania were modeled in true to life sizes to facilitate comparisons of form and function in more biologically realistic settings. Adductor muscle force loads were applied across multiple loads at the inferred muscle origination and insertion sites of the crania and mandibles, respectively. This was performed using a custom-built macro (Altair, UK) that loads multiple nodes projected towards a node(s), resulting in a vector equivalent to the line of action (Bestwick et al., 2022).

The *Saurosuchus* and *Allosaurus* models were assigned the same material properties for bone based on values for *Alligator mississippiensis* mandibular bone ($E = 15.0$ GPa, $\upsilon = 0.29$) and material properties for teeth were also based on values for *Alligator* ($E = 60.4$ GPa, $\upsilon = 0.31$; Zapata et al., 2010). All material properties within the models were treated as isotropic and homogeneous. For all feeding simulations, 5 nodes were constrained on each quadrate articular surface and 2 nodes on the occipital condyle (12 in total). The models were imported into Abaqus (Version 6.10; Simulia) for analysis and postprocessing. The following feeding-related simulations were performed:

i. Anterior bite. Bilateral biting scenario at the anterior-most premaxillary tooth. One node was constrained at the apex of the left and right tooth in all degrees of freedom.
ii. Posterior bite. Bilateral biting at the inferred posterior functional end of the snout. One node was constrained at the apexes of the left and right posterior-most maxillary tooth in *Saurosuchus* and *Allosaurus* in all degrees of freedom.

von Mises stress (a measure of overall structural strength under loading conditions; Rowe & Snively, 2022) were displayed as contour plots for both simulations to enable visual assessments of the performance of the cranium. Stresses were also measured at 10 equally spaced locations along the dorsal and palatal surfaces of the cranium to provide more detailed assessments on model performance. Measurement locations across the dorsal and palatal surfaces of all crania are shown in Figures 6 and S1.

3 | RESULTS

To facilitate comparisons between the two archosaurs, von Mises stress distributions are presented for each feeding simulation (Figures 3 and 4) and the deformation

TABLE 1 Muscle force estimates of individual jaw adductor muscles for *Saurosuchus galilei*.

Muscle	Volume (cm^3)	Length (cm)	Cross-sectional area (cm^2)	Muscle force (N)
m. AMEM	237	22.9	10.4	310.7
m. AMEP	396.3	23.7	16.7	502.1
m. AMES	425.9	21.8	19.5	584.8
m. AMP	178.4	14.8	12.1	361.9
m. PSTp	165.9	12	13.8	413.7
m. PSTs	270.5	24.1	11.2	335.9
m. PTd	133	11	12.1	362.9
m. PTv	403.2	16.9	23.8	714.3

Note: Muscle force estimates are unilateral. All values to 1 decimal place.
Abbreviations: m. AMEM, m. adductor mandibulae externus medialis; m. AMEP, m. adductor mandibulae externus profundus; m. AMES, m. adductor mandibulae superficialis; m. AMP, m. adductor mandibulae posterior; m. PSTp, m. pseudotempralis profunuds; m. PSTs, m. pseudotemporalis superficialis; m. PTd, m. pterygoideus dorsalis; m. PTv, m. pterygoideus ventralis.

plots (Figure 5) and stress values at specific measurement locations across the dorsal and palatal cranial surfaces (Figure 6) are presented with reference to taxon and feeding simulation.

At the anterior tooth constraints, *Saurosuchus* exhibited an estimated bite force of 1015 N. During the anterior bite simulation, the specimen displays high stresses in the following areas: the posterior surface of the premaxillae that borders the external nares; the quadratojugals; the articular and posterior surfaces of the quadrates; the postorbitals; the parietals; the vomers, the palatines; the ectopterygoid and the anteromedial surface of the pterygoids (Figures 3a–c and 6a). The greatest deformation is observed from the cranium rotating dorsally with the center of rotation located in the middle-posterior section of the cranium, specifically at the frontals and parietals (Figure 5a). Ventral deformation is observed from the middle section of the cranium, especially around the pterygoid where the m. pterygoideus dorsalis (m. PTd) attaches (Figure 5a). Large degrees of dorsal deformation are observed from the cranium posterior to the orbits and from the premaxillae–nasal contact

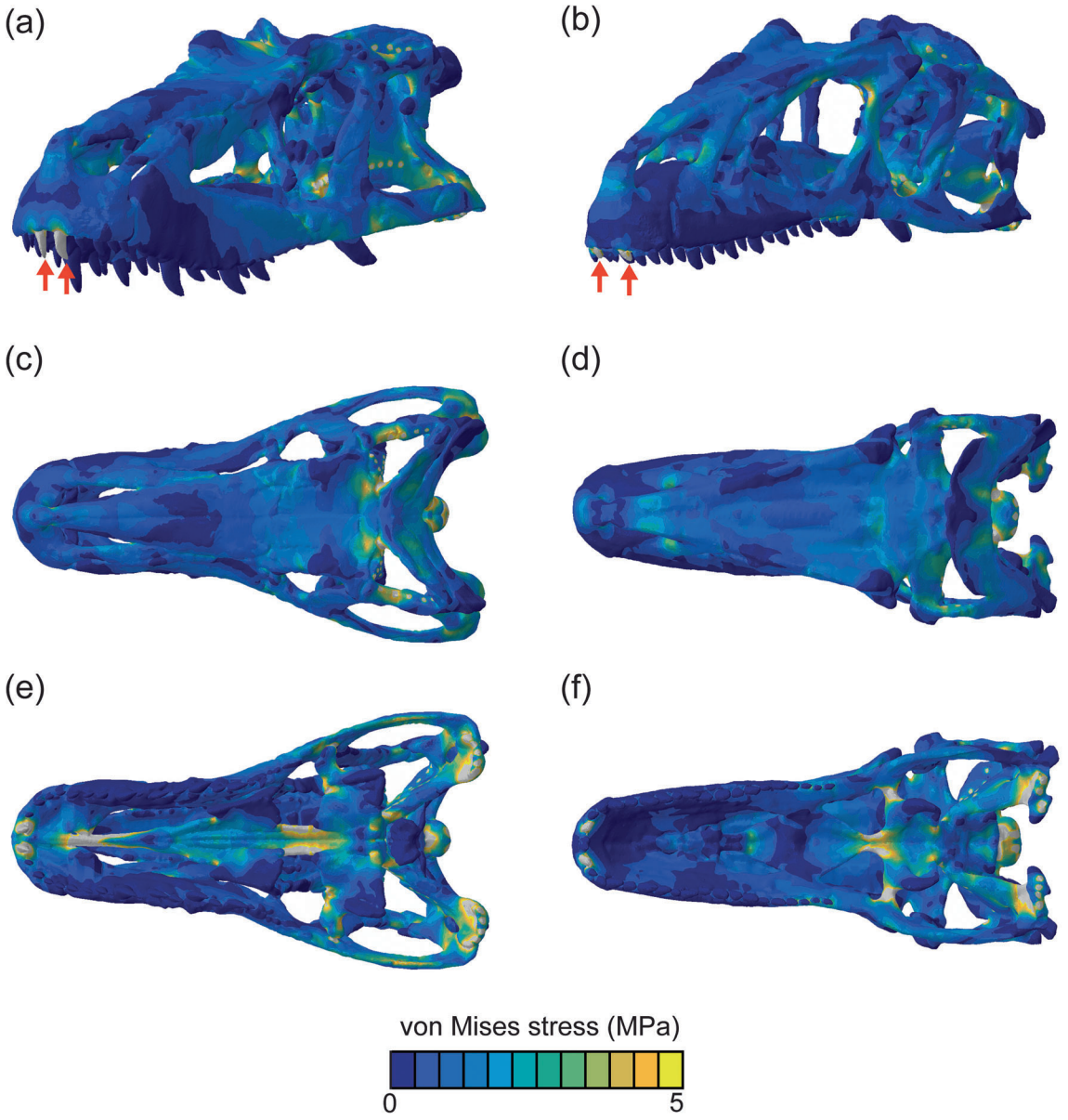

FIGURE 3 Comparisons of von Mises stress distribution of *Saurosuchus galilei* and *Allosaurus fragilis* subjected to bilateral anterior bite simulations. (a) *Saurosuchus* oblique view, (b) *Allosaurus* oblique view, (c) *Saurosuchus* dorsal view, (d) *Allosaurus* dorsal view, (e) *Saurosuchus* palatal view, and (f) *Allosaurus* palatal view. Bite positions indicated by red arrows in (a,b). The two archosaurs show generally similar stress distributions but *Saurosuchus* exhibits higher stresses around the parietals, anterior vomers and medial regions of the palatines. Models not to scale.

(Figure 5a). This contact also shifts caudally on a transverse axis, becoming level with the nasofrontal contact (Figure 5a).

The *Allosaurus* model generally displays lower stresses than the *Saurosuchus* model, especially in the vomers, parietals, and palatines of the former (Figures 3d–f and 6b). Relatively high-stress regions in the *Allosaurus* model occur in the following areas: the medial and posterior surface of the lacrimals; the ventral surface where the nasals and lacrimals meet; the lateral surface of the frontals; the dorsomedial and ventromedial surfaces of the quadrates; the ectopterygoids; and the anteromedial surface of the pterygoids (Figures 3d–f and 6b). The greatest deformation occurs at the quadratojugals, quadrates, and squamosals all rotating in a dorsoposterior direction (Figure 5b). Ventroposterior deformation is exhibited by the jugals and pterygoids and dorsal deformation is exhibited by the posterior nasal ridges and by the premaxillae–nasal contact (Figure 5b).

At the posterior tooth constraints, *Saurosuchus* exhibited an estimated bite force of 1885 N. During the posterior bite simulation, the specimen displays broadly similar stress distributions to the anterior bite model, except for lower stresses around the premaxillae,

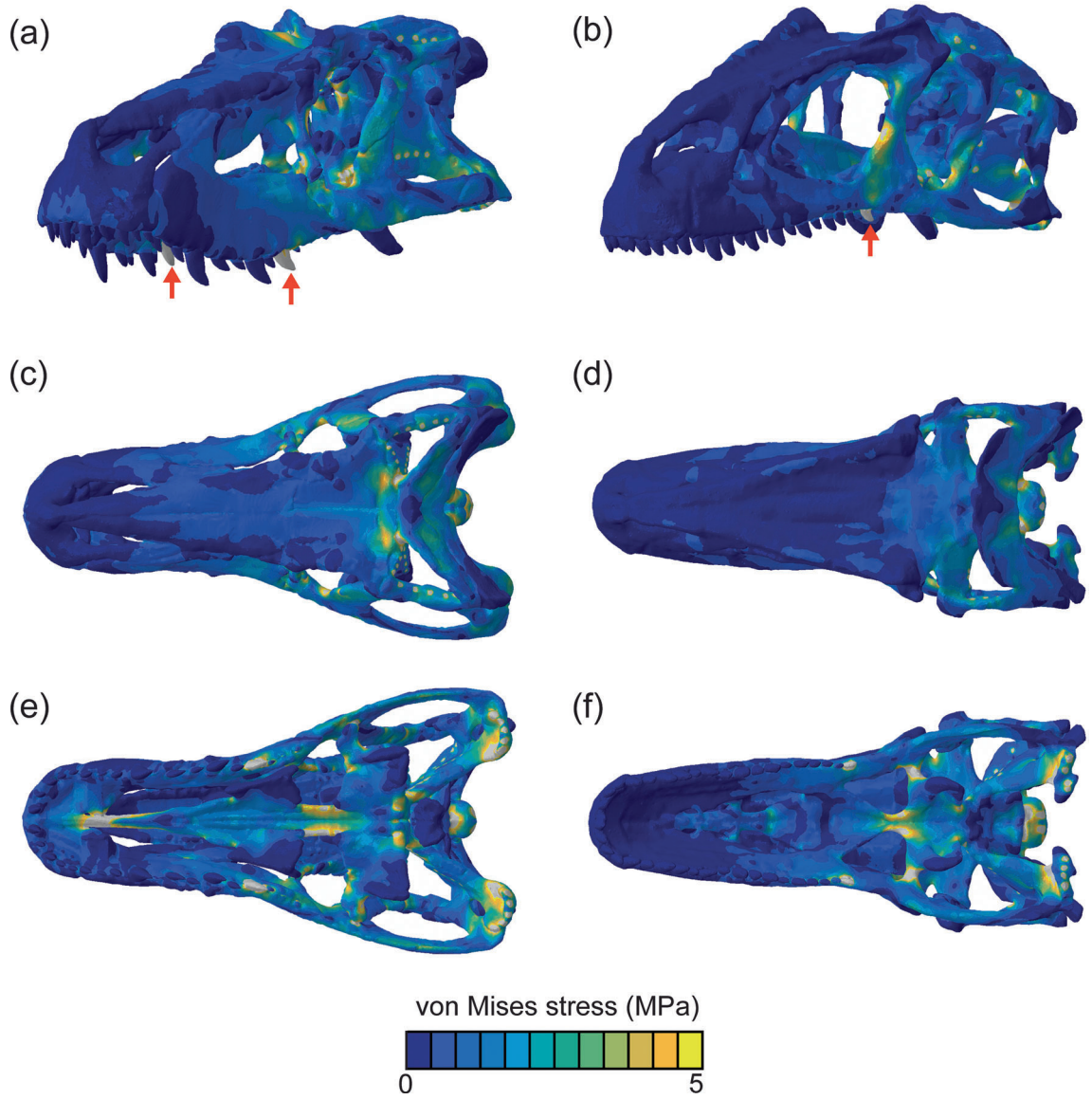

FIGURE 4 Comparisons of von Mises stress distribution of *Saurosuchus galilei* and *Allosaurus fragilis* subjected to bilateral posterior bite simulations. (a) *Saurosuchus* oblique view, (b) *Allosaurus* oblique view, (c) *Saurosuchus* dorsal view, (d) *Allosaurus* dorsal view, (e) *Saurosuchus* palatal view, and (f) *Allosaurus* palatal view. Bite positions indicated by red arrows in (a,b) (only one can be viewed for *Allosaurus* in oblique view). Both archosaurs show broadly similar stress distributions as the anterior bite simulation except for lower stresses in the premaxillae, frontals and prefrontals and higher stresses around the lacrimals and jugals. Models not to scale.

prefrontals, and frontals and higher stresses around the lacrimals and jugals (Figures 4a–c and 6a). Similar to the anterior bite simulation, deformation is observed from the cranium rotating dorsally at the frontals and parietals, although not to the same degree as in the former simulation (Figure 5a,c). Ventral deformation is also observed from the pterygoids to a larger degree than in the anterior bite simulation, and in a posterior direction around the posterior maxillae teeth (Figure 5a,c). Dorsal deformation is also observed around the nasofrontal contact (Figure 5c).

The *Allosaurus* model generally displays lower stresses in the anterior half of the cranium than both the *Saurosuchus* posterior bite and *Allosaurus* anterior bite

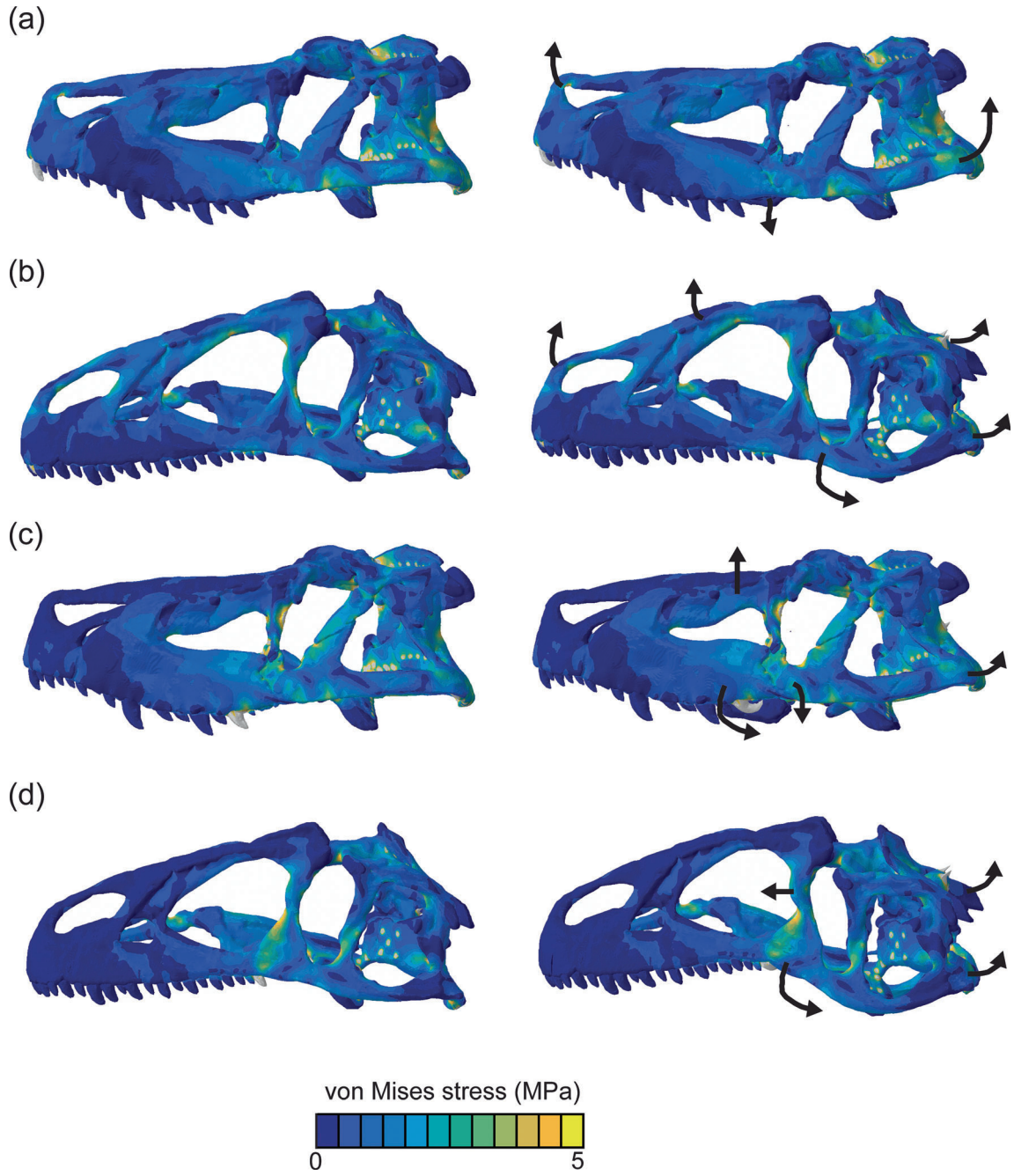

FIGURE 5 Comparisons of von Mises stress contour plots with undeformed and deformed plots from *Saurosuchus galilei* and *Allosaurus fragilis* subjected to bilateral bite simulations. (a) *Saurosuchus* anterior bite, (b) *Allosaurus* anterior bite, (c) *Saurosuchus* posterior bite, and (d) *Allosaurus* posterior bite. All models in left lateral view. Black arrows indicate the direction of deformation. Overall, *Saurosuchus* exhibits greater deformation in the anterior and central regios of the cranium, whereas *Allosaurus* exhibits greater deformation in the posterior region of the cranium. Models not to scale.

simulations (Figures 4d–f and 6b). Higher stresses than in the anterior bite simulation occur in the anterior surface of the lacrimal bars and the dorsoanterior surfaces of the jugals (Figures 4d–f and 6b). The greatest deformation is again exhibited by the quadraojugals, quadrates, and squamosals all rotating in a dorsoposterior direction (Figure 5d). Ventroposterior deformation is exhibited by the jugals and, in contrast to the anterior bite simulation, the lacrimal exhibits anterior deformation (Figure 5d).

4 | DISCUSSION

4.1 | Biomechanical modeling comparisons

Overall, the muscle reconstructions and FEA outputs indicate that *Saurosuchus* possessed a generally mechanically strong cranium. However, our results also show that *Saurosuchus* had a surprisingly weak bite for an animal of its size. The vomers, pterygoids, and quadrates are

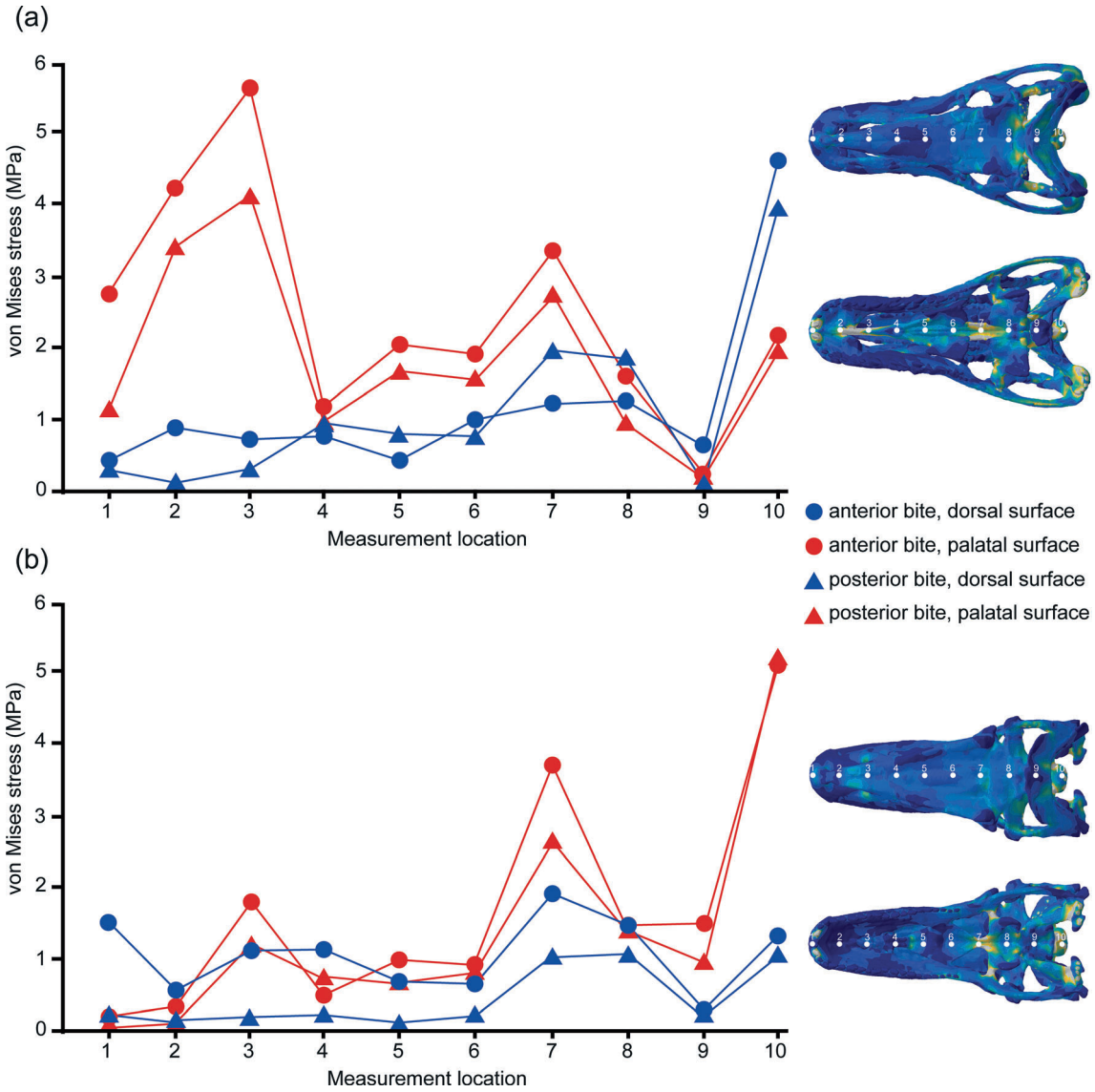

FIGURE 6 von Mises stress magnitudes of the *Saurosuchus galilei* and *Allosaurus fragilis* crania at ten locations along their dorsal and palatal surfaces, and the locations of these measurement points along the cranial surfaces, for anterior bite and posterior bite feeding simulations. (a) *Saurosuchus* values and measurement locations (dorsal surface top, palatal surface bottom). (b) *Allosaurus* values and measurement locations (dorsal surface top, palatal surface bottom). Measurement points are shown on the anterior bite simulation outputs as examples. Enlarged versions of point locations along each measured cranial surface can be found in Figure S1. The *Saurosuchus* palate generally exhibits greater stresses than the *Allosaurus* palate for both biting simulations, especially around the vomers (measurement locations 2 and 3), while stresses across the dorsal surfaces are more similar.

identified as the main areas of mechanical weakness, followed by the parietals and postorbitals. The forces exerted by the jaw muscles during feeding may therefore have been even lower than the maximum values calculated in this study. Although a well-preserved mandible would test our reconstructed muscle paths, the relatively narrow adductor chamber, the extent of the pterygoid flanges and the position of the quadrate leave little room for a deviating muscle arrangement. Furthermore, the well-preserved cranial morphology and our experimental approach enable representative interpretations from the FEA outputs and enable subsequent comparisons of these outputs with *Allosaurus*, other theropods and with modern and extinct pseudosuchians.

The juvenile condition of the modeled *Saurosuchus* has mixed impacts on observed stress distributions and deformation levels. For example, the low stresses and deformation from the parts of the premaxillae and maxillae that border the subnarial fenestrae, relative to the higher stresses exhibited from other parts of these bones indicate that these fenestrae had little impact on anterior biting behaviors. In contrast, high stresses and deformation from the quadrates corroborates earlier descriptions that the articular ends of these bones are poorly ossified, although the impact of the constraints placed on the quadrates on the observed high stresses cannot be ruled out (Alcober, 2000). The impact of the open suture between the basioccipitals and exoccipitals is difficult to assess because artificially high stresses emanate a short way into the constraint at the occipital condyle (Saint-Venant's principal: Beer & Johnston, 1992). Based on a tentative ontogenetic series of the Middle Triassic basal loricatan *Prestosuchus chiniquensis*, it is reasonable to assume that as *Saurosuchus* reached skeletal maturity, the subnarial fenestrae and basioccipital–exoccipital suture would reduce or close completely and that several elements, including the lacrimal and jugal, would thicken slightly (Alcober, 2000; Lacerda et al., 2016). Stresses in these areas may therefore be lower in adults, which would thus facilitate higher bite forces. Similar ontogenetic-based functional differences have been inferred from tyrannosaurid jaws, particularly for anterior biting scenarios (Ma et al., 2022; Rowe & Snively, 2022). However, the large size and inferred age of PVSJ 32 from histological examinations of its osteoderms (16 years old) suggest this individual did not have much more to grow (Cerda et al., 2013). Therefore, representative inferences can be made on the functional behaviors of *Saurosuchus* and basal loricatans from this studied juvenile specimen.

Model comparisons between *Saurosuchus* and *Allosaurus* show some degree of functional convergence, but also several key functional differences. Overall, the crania of both study taxa show some resistance to feeding-induced stresses and broadly similar stress distributions, particularly from the posterior halves of the crania. However, the anterior half of the *Allosaurus* cranium can be argued as notably mechanically stronger, especially with regards to the anterior palate. Furthermore, the *Saurosuchus* posterior bite force of less than half that of previous *Allosaurus* estimates from the same jaw position (around 3500 N; Rayfield et al., 2001), which is itself considered rather weak for a ~7.5 m long theropod (Lautenschlager, 2015; Paul, 2016). These functional differences could be explained by several subtle, yet important, morphological differences between the study taxa. For example, *Saurosuchus* has a somewhat rectangular shaped cranium when observed in lateral view, with the ventral edge of the maxillae slightly convex in shape (Alcober, 2000; Sill, 1974), in contrast to the rounded anterior and posterior ends of the *Allosaurus* cranium with the ventral maxillae edges being slightly concave (Madsen, 1976; Snively et al., 2013). This could explain the larger degrees of anterior deformation in *Saurosuchus* during the anterior biting simulation. Furthermore, the *Saurosuchus* vomers are much thinner than in *Allosaurus*, which is the likely cause of the higher observed stresses from the palate of the pseudosuchian during both biting simulations. These results provide another example where similar form between distantly related extinct taxa does not equate to the same functional morphologies (Bestwick et al., 2022; Ferry-Graham et al., 2002; Fisher, 1985; Lautenschlager et al., 2016; Thomason, 1995).

Although not directly studied here, the *Saurosuchus* FEA results can also be broadly compared with other theropods and modern crocodilians. For example, *Saurosuchus* bite forces are a fraction of forces estimated for *Tyrannosaurus rex* (around 17,000 N and 34,500 N from anteriorly and posteriorly positioned biting simulations respectively; Gignac & Erickson, 2017), further highlighting functional differences between Triassic and post-Triassic apex predators. Recorded bite forces of modern crocodilians show that *Saurosuchus* bite forces are most similar to gharials (*Gavialis gangeticus*; 924 N and 1895 N for anterior and posterior bite forces, respectively), which coincidentally also have relatively weak bites for their size (3–3.5 m total length; Erickson et al., 2012). In fact, all modern crocodilians with total body lengths of >2 m have stronger anterior and posterior bite forces than *Saurosuchus* (Erickson et al., 2012). This is not surprising given crocodilians have among the highest recorded bite forces of any modern animal (Erickson et al., 2003, 2012), and whose skulls are adapted to resist high feeding-generated forces (Bestwick et al., 2022; McHenry et al., 2006; Montefeltro et al., 2020; Walmsley et al., 2013). These

characteristics therefore indicate a limited phylogenetic signal in the functional morphology of modern and extinct pseudosuchians.

4.2 | Possible feeding behaviors of *Saurosuchus* and basal loricatans

Based on morphological adaptations and the functional evidence presented here, we do not doubt the hypothesis that *Saurosuchus*, and basal loricatans in general, were carnivores (Chatterjee, 1985; Gower & Schoch, 2009; Mastrantonio et al., 2019; Nesbitt, 2011; Nesbitt et al., 2013; Roberto-Da-Silva et al., 2018). However, questions remain concerning how basal loricatans procured prey and the feeding behaviors they exhibited. For example, they were unlikely to have been obligate scavengers as their large size and the diversity of smaller, contemporaneous terrestrial carnivores (ornithosuchids, crocodylomorphs, theropods, and therapsid cynodonts) would have made carrion an unreliable exclusive food source (Carbone et al., 2011; Ezcurra et al., 2017; Martínez et al., 2013; Nesbitt et al., 2013). Regular osteophagy is unlikely for two main reasons: (i) *Saurosuchus* does not possess the incredibly high bite forces needed to crack bones as deployed by tyrannosaurids and modern crocodilians (Erickson et al., 2012, 2014; Gignac & Erickson, 2017; Meers, 2002; Therrien et al., 2005), although small bones could have potentially been swallowed whole; (ii) *Saurosuchus* does not possess morphological features that typically facilitate bone cracking and shearing. For example, spotted hyenas have lower bite forces than African lions but their robust carnassial teeth and their enlarged zygomatic arches and sagittal crests for larger adductor muscle attachment areas all aid in producing the necessary tooth pressures to crack bone (Christiansen & Adolfssen, 2005; Christiansen & Wroe, 2007; Schubert et al., 2010).

An alternative feeding behavior involves defleshing carcasses via scraping or biting off muscle tissue from procured prey. Such a behavior is hypothesized for *Allosaurus* (Lautenschlager, 2015; Rayfield, 2005; Rayfield et al., 2001; Snively et al., 2013), and is also exhibited by the Komodo dragon (*Varanus komodoensis*), a large extant reptile that possesses ziphodont dentitions like those of basal loricatans and theropods (D'Amore & Blumenschine, 2009, 2012; Mujal et al., 2022; Whitney et al., 2020). However, defleshing can involve varying levels of tooth–bone interactions between carnivores. For example, modern cheetahs (*Acinoynx jubatus*) actively avoid bone during defleshing in contrast to lions and hyenas (Hayward et al., 2006; Schubert et al., 2010; van Valkenburgh, 1996; van Valkenburgh et al., 1990). Based on macroscopic tooth wear patterns and bite marks on contemporaneous taxa (including from conspecifics), the Middle Triassic basal loricatan *Batrachotomus* shows relatively high degrees of bone interactions during defleshing compared with some similarly sized theropods (e.g., megalosauroids; Mujal et al., 2022). More specifically, *Batrachotomus* is inferred to have primarily used the premaxillary teeth during defleshing (Mujal et al., 2022). *Allosaurus* similarly shows high degrees of presumably feeding-related tooth–bone interactions that suggest it too preferred to use its premaxillary teeth for defleshing (Drumheller et al., 2020; Hone & Rauhut, 2010; Mujal et al., 2022). Although premaxillary teeth are unknown from *Saurosuchus*, the stress magnitudes and deformation levels around the nasal bridge from the anterior bite scenario indicate that defleshing in this way was perhaps less likely for this basal loricatan. Generally, lower stresses from the posterior bite scenario suggest that the posterior teeth in contrast may have been used for defleshing by *Saurosuchus*. However, the few known well-preserved distal *Saurosuchus* teeth show less macroscopic wear than distal *Batrachotomus* teeth (Alcober, 2000; Mujal et al., 2022; Sill, 1974). *Saurosuchus* may therefore have more readily avoided bone compared with *Batrachotomus* and *Allosaurus* and prioritized less tough parts of carcasses during feeding.

Although only fragmentarily preserved, the mandible of *Saurosuchus* provides further indications for a comparatively weak bite and a nonosteophagous behavior. In tyranosauroids and other large carnivorous theropods, structural strengthening evolved in the mandible in the form of an expansion of the post-dentary region and a dorsally curving (=upturned) dentary, often accompanied by symphyseal expansion (Ma et al., 2022). Similar morphologies are present in some loricatans, such as *Batrachotomus*, *Prestosuchus*, and *Postosuchus* (Nesbitt et al., 2013). In contrast, the preserved tip of the mandible in *Saurosuchus* does not show any expansion or dorsal curvature (although the preserved elements preclude a full assessment). *Batrachotomus* and *Postosuchus* further show extensive buttressing of the maxillary and jugal region, mirrored by a similar shelf on the surangular (Gower, 1999; Nesbitt et al., 2013; Weinbaum, 2011). Such a shelf/buttressing is absent in the skull of *Saurosuchus* suggesting the corresponding shelf may have been absent on the surangular as well. It is therefore possible that *Saurosuchus* lacked the morphofunctional modifications associated with osteophagy and large bite forces and had a more "gracile" mandibular and overall cranial morphology compared with other loricatans.

4.3 | Functional and ecological convergence between basal loricatans and theropods

Our biomechanical modeling demonstrates that the functional morphology of *Saurosuchus* somewhat differs to that of medium and large-sized theropods, and thus indicates that degrees of convergence between basal loricatans and post-Triassic theropods may not have been as strong as previously hypothesized (Alcober, 2000; Chatterjee, 1985; Gower, 2000; Klein et al., 2017; Mastrantonio et al., 2019; Mujal et al., 2022; Nesbitt et al., 2013; Roberto-Da-Silva et al., 2018; Weinbaum, 2011, 2013). More broadly, our results also highlight that the classification of taxa as apex predators without considering their functional repertoires is simplistic and limits understanding of their exact ecological role(s) within food webs. Characteristics of food webs in which morphologically convergent predators live influence likelihoods of functional and ecological convergence between distantly related predators. For example, the low bite force of *Saurosuchus* relative to post-Triassic theropods could be explained by size differences of contemporaneous prey. During the Middle Triassic and early Late Triassic (Carnian–early Norian) average carnivore size exceeded herbivore size, in contrast to the rest of the Mesozoic (Sookias et al., 2012; Turner & Nesbitt, 2013). Basal loricatans were thus often the largest terrestrial animals in their environment during this time frame (Sookias et al., 2012; Turner & Nesbitt, 2013). In the case of *Saurosuchus*, for example, the only other similarly sized terrestrial taxon (i.e., >250 kg) from the same biozones of the Ischigualasto Formation is the dicynodont therapsid *Ischigualastia jenseni* (Cox, 1962; Martínez et al., 2013). In contrast, *Allosaurus* with an estimated length of around 7.5 m is contemporaneous with several sauropod species from the Morrison Formation that attained sizes of 20–25 m (Mannion et al., 2021; Paul, 2016; although *Allosaurus* more likely predated upon smaller juveniles; Paul, 1988). It is therefore possible that basal loricatans did not need a strong bite typical of similarly sized theropods (or of modern pseudosuchians) to procure and process prey much smaller than themselves. It is also possible that stronger bites could have evolved in later-occurring basal loricatans with larger contemporaneous herbivores. For example, *Fasolasuchus tenax* size (8+ m long; no reliable body mass estimates exist) from the middle-late Norian Los Colorados Formation, Argentina, is exceeded by the sauropodomorph *Lessemsaurus sauropoides* (upper mass estimate of 10 tons, no length estimates exist; Apaldetti et al., 2018; Bonaparte, 1981; Nesbitt et al., 2013; Pol & Powell, 2007). However, the lack of three-dimensionally preserved skull material from this basal loricatan prevents robust functional investigations (Bonaparte, 1981; Nesbitt et al., 2013). Nevertheless, our results show functional, as well as ecological, differences between archosaurian carnivores from Triassic and post-Triassic food webs.

Our results, along with morphological and functional data of other contemporaneous carnivorous archosaurs provide novel, yet tentative, insight into the functioning of some Middle and Late Triassic food webs. For example, ornithosuchids likely filled mesopredator and/or scavenger niches based on their medium size (~2 m long), being identified as the perpetrators of bite-marks on rhynchosaur bones and biomechanical investigations revealing they had intermediately powerful, yet slow, bites (von Baczko, 2018; Benton, 1983; Walker, 1964). It is tempting to suggest that if *Saurosuchus*, and possibly other basal loricatans, minimized tooth–bone interactions during feeding, the resulting wastage would have produced abundant carrion that could have supported a variety of distantly related Triassic mesopredators/scavengers (von Baczko, 2018; DeVault et al., 2003; Martínez et al., 2013; Wilkenros et al., 2013). Resource partitioning between Triassic carnivores was therefore potentially based on a combination of both size and functional differences.

5 | CONCLUSIONS

Our study shows that despite the morphological similarity between the crania of basal loricatans and theropods, several key functional differences occurred between the studied representatives. *Saurosuchus* had a weak bite for an animal of its size and possessed several mechanically weak features, such as the vomers and pterygoids that disproportionately influenced the functional behaviors that could have been performed by its otherwise mechanically strong cranium. *Saurosuchus* therefore perhaps fed by defleshing carcasses with its posteriorly positioned its teeth, while minimizing tooth–bone interactions, with osteophagy very unlikely. This is in marked contrast to the feeding behaviors inferred from similarly sized theropods, showcasing previously unappreciated functional disparity between hypothesized Triassic and post-Triassic carnivores. Our results also contrast with the inferred feeding behaviors of other basal loricatans, providing novel insight into the functional diversity of this pseudosuchian group. The inferred functional morphology of *Saurosuchus* indicates it was perhaps rather wasteful at carcasses and was therefore a keystone species of the Late Triassic ecosystem in which it lived, regulating the populations of both herbivores and mesopredators through direct predation and carrion production respectively.

AUTHOR CONTRIBUTIONS

Molly J. Fawcett: Methodology; software; data curation; writing – review and editing; investigation; formal analysis; funding acquisition; visualization. **Stephan Lautenschlager:** Conceptualization; methodology; software; writing – review and editing; supervision; project administration; validation; funding acquisition; resources. **Jordan Bestwick:** Writing – original draft; visualization; supervision; validation; data curation; methodology; formal analysis; project administration. **Richard J. Butler:** Writing – review and editing; conceptualization; supervision; funding acquisition; methodology; project administration.

ACKNOWLEDGMENTS

Thanks to Matthew Colbert and Richard Ketcham who conducted the original scans of PVSJ 32 available on Digimorph and to Julia Desojo and Martín Ezcurra for providing additional photographs of the specimen. This study started as an MSc (by Research) project by M.F. and was completed with support from a Leverhulme Trust Research Project Grant (RPG-2019-364) to Richard J. Butler, Stephan Lautenschlager, Paul Barrett, and Laura Porro. Thanks to Manabu Sakamoto, Ivan Sansom, Adam Hartstone-Rose, and two anonymous reviewers for helpful comments on an earlier version of the article.

FUNDING INFORMATION

Leverhulme Trust (Grant number: RPG-2019-364).

CONFLICT OF INTEREST STATEMENT

We declare no competing interests.

DATA AVAILABILITY STATEMENT

The original scan data for the *Saurosuchus* cranium are freely available on Digimorph (http://www.digimorph.org/specimens/Saurosuchus_galilei/).

ORCID

Stephan Lautenschlager https://orcid.org/0000-0003-3472-814X
Jordan Bestwick https://orcid.org/0000-0002-1098-6286
Richard J. Butler https://orcid.org/0000-0003-2136-7541

REFERENCES

Alcober, O. (2000). Redescription of the skull of *Saurosuchus galilei* (Archosauria: Rauisuchidae). *Journal of Vertebrate Paleontology*, *20*, 302–316.

Apaldetti, C., Martínez, R. N., Cerda, I. A., Pol, D., & Alcober, O. (2018). An early trend towards gigantism in Triassic sauropodomorph dinosaurs. *Nature Ecology & Evolution*, *2*, 1227–1232.

von Baczko, M. B. (2018). Rediscovered cranial material of *Venaticosuchus rusconii* enables the first jaw biomechanics in Ornithosuchidae (Archosauria: Pseudosuchia). *Ameghiniana*, *55*, 365–379.

Bates, K. T., & Falkingham, P. L. (2018). The importance of muscle architecture in biomechanical reconstructions of extinct animals: A case study using *Tyrannosaurus rex*. *Journal of Anatomy*, *233*, 625–635.

Beer, F. P., & Johnston, E. R. (1992). *Mechanics of materials*. McGraw-Hill.

Benton, M. J. (1983). The Triassic reptile *Hyperodapedon* from Elgin: Functional morphology and relationships. *Philosophical Transactions of the Royal Society B*, *302*, 605–720.

Bestwick, J., Jones, A. S., Nesbitt, S. J., Lautenchlager, S., Rayfield, E. J., Cuff, A. R., Barrett, P. M., Porro, L. B., & Butler, R. J. (2022). Cranial functional morphology of the pseudosuchian *Effigia* and implications for its ecological role in the Triassic. *The Anatomical Record*, *305*, 2435–2462.

Bonaparte, J. F. (1981). Descripcion de *Fasolasuchus tenax* y su significado en la sistematica y evolucion de los Thecodontia. *Revista del Museo Argentino de Ciencias Naturales 'Bernardino Rivadavia'*, *3*, 55–101.

Brink, K. S., Reisz, R. R., LeBlanc, A. R. H., Chang, R. S., Lee, Y. C., Chiang, C.-C., Huang, T., & Evans, D. C. (2015). Developmental and evolutionary novelty in the serrated teeth of theropod dinosaurs. *Scientific Reports*, *5*, 12338.

Brusatte, S. L., Benton, M. J., Lloyd, G. T., Ruta, M., & Wang, S. C. (2010). Macroevolutionary radiation of archosaurs (Tetrapoda: Diapsida). *Earth and Environmental Science Transactions of the Royal Society of Edinburgh*, *101*, 367–382.

Brusatte, S. L., Benton, M. J., Ruta, M., & Lloyd, G. T. (2008). Superiority, competition and opportunism in the evolutionary radiation of dinosaurs. *Science*, *321*, 1485–1488.

Brusatte, S. L., Butler, R. J., Sulej, T., & Niedźwiedzki, G. (2009). The taxonomy and anatomy of rauisuchian archosaurs from the Late Triassic of Germany and Poland. *Acta Palaeontologica Polonica*, *54*, 221–230.

Butler, R. J., Fernandez, V., Nesbitt, S. J., Leite, J. V., & Gower, D. J. (2022). A new pseudosuchian archosaur, *Mambawakale ruhuhu* gen. et sp. nov., from the Middle Triassic Manda Beds of Tanzania. *Royal Society Open Science*, *9*, 211622.

Carbone, C., Turvey, S. T., & Bielby, J. (2011). Intra-guild competition and it simplications for one of the biggest terrestrial predators, *Tyrannosaurus rex*. *Proceedings of the Royal Society B-Biological Sciences*, *278*, 2682–2690.

Cerda, I. A., Desojo, J. B., Scheyer, T. M., & Schultz, C. L. (2013). Osteoderm microstructure of "rauisuchian" archosaurs from South America. *Geobios*, *46*, 273–283.

Chatterjee, S. (1985). *Postosuchus*, a new thecodontian reptile from the Triassic of Texas and the origin of tyrannosaurs. *Philosophical Transactions of the Royal Society of London B*, *309*, 395–460.

Chin, K., Tokaryk, T. T., Erickson, G. M., & Calk, L. C. (1998). A king-sized theropod coprolite. *Nature*, *393*, 680–682.

Christiansen, P., & Adolfssen, J. S. (2005). Bite forces, canine strength and skull allometry in carnivores (Mammalia, Carnivora). *Journal of the Zoological Society of London*, *266*, 133–151.

Christiansen, P., & Wroe, S. (2007). Bite forces and evolutionary adaptations to feeding ecology in carnivores. *Ecology*, *88*, 347–358.

Chure, D. J., & Loewen, M. A. (2020). Cranial anatomy of *Allosaurus jimmadseni*, a new species from the lower part of the

Morrison Formation (Upper Jurassic) of Western North America. *PeerJ*, *8*, e7803.

Cost, I. N., Middleton, K. M., Sellers, K. C., Echols, M. S., Witmer, L. M., Davis, J. L., & Holliday, C. M. (2020). Palatal biomechanics and its significance for cranial kinesis in *Tyrannosaurus rex*. *The Anatomical Record*, *303*, 999–1017.

Cox, C. B. (1962). Preliminary diagnosis of *Ischigualastia*, a new genus of dicynodont from Argentina. *Breviora*, *156*, 8–9.

D'Amore, D. C., & Blumenschine, R. J. (2009). Komodo monitor (*Varanus komodoensis*) feeding behaviour and dental function reflected through tooth marks on bone surfaces, and the application to ziphodont paleobiology. *Paleobiology*, *35*, 525–552.

D'Amore, D. C., & Blumenschine, R. J. (2012). Using striated tooth marks on bone to predict body size in theropod dinosaurs: A model based on feeding observations of *Varanus komodoensis*, the Komodo monitor. *Paleobiology*, *38*, 79–100.

DeSantis, L. R. G., Scott, J. R., Schubert, B. W., Donohue, S. L., McCray, B. M., Stolk, C. A., van Winburn, A. A., Greshko, M. A., & O'Hara, M. C. (2013). Direct comparisons of 2D and 3D dental microwear proxies in extant herbivorous and carnivorous mammals. *PLoS One*, *8*, e71428.

Desojo, J. B., Heckert, A. B., Martz, J. W., Parker, W. G., Schoch, R. R., Small, B. J., & Sulej, T. (2013). Aetosauria: A clade of armoured pseudosuchians from the Upper Triassic continetnal beds. In S. J. Nesbitt, J. B. Desojo, & R. B. Irmis (Eds.), *Antomy, phylogeny and palaeobiology of early archosaurs and their kin* (Vol. 379, pp. 203–239). Geological Society.

Desojo, J. B., von Baczko, M. B., & Rauhut, O. W. M. (2020). Anatomy, taxonomy and phylogenetic relationships of *Prestosuchus chiniquensis* (Archosauria: Pseudosuchia) from the original collection of von Huene, Middle-Late Triassic of southern Brazil. *Palaeontologia Electronica*, *23*, a04.

DeVault, T. L., Rhodes, J. O. E., & Shivik, J. A. (2003). Scavenging by vertebrates: Behavioral, ecological, and evolutionary perspectives on an important energy transfer pathway in terrestrial ecosystems. *Oikos*, *102*, 225–234.

Drumheller, S. K., McHugh, J. B., Kane, M., Riedel, A., & D'Amore, D. C. (2020). High frequencies of theropod bite marks provide evidence for feeding, scavenging, and possible cannibalism in a stressed Late Jurassic ecosystem. *PLoS One*, *15*, e0233115.

Erickson, G. M., Gignac, P. M., Lappin, A. K., Vliet, K. A., Brueggen, J. D., & Webb, G. J. W. (2014). A comparative analysis of ontogenetic bite-force scaling among Crocodylia. *Journal of Zoology*, *292*, 48–55.

Erickson, G. M., Gignac, P. M., Steppan, S. J., Lappin, A. K., Vliet, K. A., Brueggen, J. D., Inouye, B. D., Kledzik, D., & Webb, G. J. (2012). Insights into the ecology and evolutionary success of crocodilians revealed through bite-force and tooth-pressure experimentation. *PLoS One*, *7*, e31781.

Erickson, G. M., Lappin, A. K., & Vliet, K. A. (2003). The ontogeny of bite-force performance in American alligator (*Alligator mississippiensis*). *Journal of Zoology*, *260*, 317–327.

Ezcurra, M. D., Fiorelli, L. E., Martinelli, A. G., Rocher, S., von Baczko, M. B., Ezpeleta, M., Tarborda, J. R. A., Hechenleitner, E. M., Trotteyn, M. J., & Desojo, J. B. (2017). Deep faunistic turnovers preceded the rise of dinosaurs in southwestern Pangea. *Nature Ecology & Evolution*, *1*, 1477–1483.

Ferry-Graham, L. A., Bolnick, D. I., & Wainwright, P. C. (2002). Using functional morphology to examine the ecology and evolution of specialization. *Integrative and Comparative Biology*, *42*, 265–277.

Fisher, D. C. (1985). Evolutionary morphology: Beyond the analogous, the anecdotal and the ad hoc. *Paleobiology*, *11*, 120–138.

França, M. A. G., Ferigolo, J., & Langer, M. C. (2011). Associated skeletons of the new middle Triassic "Rauisuchian" from the Brazil. *Naturwissenschaften*, *98*, 389–395.

Garcia, M. S., Müller, R. T., Pretto, F. A., Da-Rosa, Á. A. S., & Dias-da-Silva, S. (2021). Taxonomic and phylogenetic reassessment of a large-bodied dinosaur from the earliest dinosaur-bearing beds (Carnian, Upper Triassic) from southern Brazil. *Journal of Systematic Palaeontology*, *19*, 1–37.

Gignac, P. M., & Erickson, G. M. (2017). The biomechanics behind extreme osteophagy in *Tyrannosaurus rex*. *Scientific Reports*, *7*, 1–10.

Gower, D. J. (1999). Cranial osteology of a new rauisuchian archosaur from the Middle Triassic of southern Germany. *Stuttgarter Beiträge zur Naturkunde B*, *280*, 1–49.

Gower, D. J. (2000). Rauisuchian archosaurs (Reptilia, Diapsida): An overview. *Neues Jahrbuch für Geologie und Paläontologie*, *218*, 447–488.

Gower, D. J., & Schoch, R. R. (2009). Postcranial anatomy of the rauisuchian archosaur *Batrachotomus kupferzellensis*. *Journal of Vertebrate Paleontology*, *29*, 103–122.

Hayward, M. W., O'Brien, J., Hofmeyer, M., & Kerley, G. I. H. (2006). Prey preferences of the cheetah (*Acinonyx jubatus*) (Felidae: Carnivora): Morphological limitations or the need to capture rapidly consumable prey before kleptoparasites arrive? *Journal of the Zoological Society of London*, *270*, 615–627.

Holliday, C. M. (2009). New insights into dinosaur jaw muscle anatomy. *The Anatomical Record*, *229*, 1246–1265.

Hone, D. W. E., & Rauhut, O. W. M. (2010). Feeding behaviour and bone utilization by theropod dinosaurs. *Lethaia*, *43*, 232–244.

Klein, N., Foth, C., & Schoch, R. R. (2017). Preliminary observations on the bone of the Middle Triassic pseudosuchian archosaur *Batrachotomus kupferzellensis* reveal fast growth with laminar fibrolamellar bone tissue. *Journal of Vertebrate Paleontology*, *37*, e1333121.

Lacerda, M. B., Mastrantonio, B. M., Fortier, D. C., & Schultz, C. L. (2016). New insights on *Prestosuchus chiniquensis* Huene, 1942 (Pseudosuchia, Loricata) based on new specimens form the "Tree Sanga" Outcrop, Chiniquá Region, Rio Grande do Sul, Brazil. *PeerJ*, *4*, e1622.

Lautenschlager, S. (2013). Cranial myology and bite force performance of *Erlikosaurus andrewsi*: A novel approach for digital muscle reconstructions. *Journal of Anatomy*, *222*, 260–272.

Lautenschlager, S. (2015). Estimating cranial musculoskeletal constraints in theropod dinosaurs. *Royal Society Open Science*, *2*, 150495.

Lautenschlager, S. (2016). Reconstructing the past: Methods and techniques for the digital restoration of fossils. *Royal Society Open Science*, *3*, 160342.

Lautenschlager, S., Brassey, C. A., Button, D. J., & Barrett, P. M. (2016). Decoupled form and function in disparate herbivorous dinosaur clades. *Scientific Reports*, *6*, 26495.

Ma, W., Pittman, M., Butler, R. J., & Lautenschlager, S. (2022). Macroevolutionary trends in theropod feeding mechanics. *Current Biology*, *32*, 677–686.e673.

Madsen, J. H. (1976). *Allosaurus fragilis*: A revised osteology. *Utah Geological and Mining Survey Bulletin*, *109*, 1–163.

Mannion, P. D., Tschopp, E., & Whitlock, J. A. (2021). Anatomy and systematics of the diplodocid *Amphicoelias altus* supports high sauropod dinosaur diversity in the Upper Jurassic Morrison Formation of the USA. *Royal Society Open Science*, *8*, 210377.

Martínez, R. N., Apaldetti, C., Alcober, O. A., Colombi, C. E., Sereno, P. C., Fernandez, E., Malnis, P. S., Correa, G. A., & Abelin, D. (2013). Vertebrate succession in the Ischigualasto Formation. *Journal of Vertebrate Paleontology*, *32*, 10–30.

Mastrantonio, B. M., von Baczko, M. B., Desojo, J. B., & Schultz, C. L. (2019). The skull anatomy and cranial endocast of the pseudosuchid archosaur *Prestosuchus chiniquensis* from the Triassic of Brazil. *Acta Palaeontologica Polonica*, *64*, 171–198.

McHenry, C. R., Clausen, P. D., Daniel, W. J. T., Meers, M. B., & Pendharkar, A. (2006). Biomechanics of the rostrum in crocodilians: A comparative analysis using finite-element modeling. *The Anatomical Record*, *288*, 827–849.

Meers, M. B. (2002). Maximum bite force and prey size of *Tyrannosaurus rex* and their relationships to the inference of feeding behaviour. *Historical Biology*, *16*, 1–12.

Montefeltro, F. C., Lautenchlager, S., Godoy, P. L., Ferreira, G. S., & Butler, R. J. (2020). A unique predator in a unique ecosystem: Modelling the apex predator within a Late Cretaceous crocodyliform-dominated fauna from Brazil. *Journal of Anatomy*, *237*, 323–333.

Mujal, E., Foth, C., Maxwell, E. E., Seegis, D., & Schoch, R. R. (2022). Fedding habits of the Middle Triassic pseudosuchian *Batrachotomus kupferzellensis* from Germany and palaeoecological implications for archosaurs. *Palaeontology*, *65*, e12597.

Nesbitt, S. J. (2007). The anatomy of *Effigia okeeffeae* (Archosauria, Suchia), theropod-like convergence, and the distribution of related taxa. *Bulletin of the American Museum of Natural History*, *302*, 1–84.

Nesbitt, S. J. (2011). The early evolution of archosaurs: Relationships and the origin of major clades. *Bulletin of the American Museum of Natural History*, *352*, 1–292.

Nesbitt, S. J., Brusatte, S. L., Desojo, J. B., Liparini, A., De França, M. A. G., Weinbaum, J. C., & Gower, D. J. (2013). Rauisuchia. In S. J. Nesbitt, J. B. Desojo, & R. B. Irmis (Eds.), *Anatomy, phylogeny and palaeobiology of early archosaurs and their Kin* (Vol. 379, pp. 241–274). Geological Society.

Nesbitt, S. J., & Desojo, J. B. (2017). The osetology and phylogenetic position of *Luperosuchus fractus* (Archosauria: Loricata) from the latest Middle Triassic or earliest Late Triassic of Argentina. *Ameghiniana*, *54*, 261–282.

Nesbitt, S. J., & Norell, M. A. (2006). Extreme convergence in the body plans of an early suchian (Archosauria) and ornithomimid dinosaurs (Theropoda). *Proceedings of the Royal Society B-Biological Sciences*, *273*, 1045–1048.

Ogada, D. L., Torchin, M. E., Kinnaird, M. F., & Ezenwa, V. O. (2012). Effects of vulture declines on facultative scavengers and potential implications for mammalian disease transmission. *Conservation Biology*, *326*, 453–460.

Parker, W. G., Nesbitt, S. J., Irmis, R. B., Martz, J. W., Marsh, A. D., Brown, M. A., Stocker, M. R., & Werning, S. (2021). Osteology and relationships of *Revueltosaurus callenderi* (Archosauria: Suchia) from the Upper Triassic (Norian) Chinle Formation of Petrified Forest National Park, Arizona, United States. *The Anatomical Record*, *305*, 2353–2414.

Paul, G. S. (1988). *Predatory Dinosaurs of the World*. Simon and Schuster.

Paul, G. S. (2016). *The Princeton Field Guide to Dinosaurs* (2nd ed.). Princeton University Press.

Pol, D., & Powell, J. E. (2007). New information on *Lessemsaurus sauropoides* (Dinosauria: Sauropodomorpha) from the Upper Triassic of Argentina. *Special Papers in Palaeontology*, *77*, 223–243.

Rahman, I. A., & Lautenchlager, S. (2016). Applications of three-dimensional box modelling to paleontological functional analysis. *The Paleontological Society Papers*, *22*, 119–132.

Rayfield, E. J. (2004). Cranial mechanics and feeding in *Tyrannosaurus rex*. *Proceedings of the Royal Society B-Biological Sciences*, *271*, 1451–1459.

Rayfield, E. J. (2005). Aspects of comparative cranial mechanics in the theropod dinosaurs *Coelophysis*, *Allosaurus* and *Tyrannosaurus*. *Zoological Journal of the Linnean Society*, *144*, 309–316.

Rayfield, E. J., Norman, D. B., Horner, C. C., Horner, J. R., Smith, P. M., Thomanson, J. J., & Upchurch, P. (2001). Cranial design and function in a large theropod dinosaur. *Nature*, *409*, 1033–1037.

Roberto-Da-Silva, L., Müller, R. T., França, M. A. G., Cabreira, S. F., & Dias-da-Silva, S. (2018). An impressive skeleton of the giant top predator *Prestosuchus chiniquensis* (Pseduosuchia: Loricata) from the Triassic of Southern Brazil, with phylogenetic remarks. *Historical Biology*, *32*, 976–995.

Rowe, A. J., & Snively, E. (2022). Biomechanics of juvenile tyrannosaurid mandibles and their implications for bite force: Evolutionary biology. *The Anatomical Record*, *305*, 373–392.

Sakamoto, M. (2010). Jaw biomechanics and the evolution of biting performance in theropod dinosaurs. *Proceedings of the Royal Society B-Biological Sciences*, *277*, 3327–3333.

Schubert, B. W., & Ungar, P. S. (2005). Wear facets and enamel spalling in tyrannosaurid dinosaurs. *Acta Palaeontologica Polonica*, *50*, 93–99.

Schubert, B. W., Ungar, P. S., & DeSantis, L. R. G. (2010). Carnassial microwear and dietary behaviour in large carnivorans. *Journal of Zoology*, *280*, 257–263.

Sill, W. D. (1974). The anatomy of *Saurosuchus galilei* and the relationships of the rauisuchid thecodonts. *Bulletin of the Museum of Comparative Zoology*, *146*, 317–362.

Sinclair, A. R. E., Mduma, S., & Brashares, J. S. (2003). Patterns of predation in a diverse predator–prey system. *Nature*, *425*, 288–290.

Snively, E., Cotton, J. R., Ridgely, R., & Witmer, L. M. (2013). Multibody dynamics model of head and neck function in *Allosaurus* (Dinosauria, Theropoda). *Palaeontologia Electronica*, *16*, 11A.

Snively, E., & Russell, A. R. (2007). Craniocervical feeding dynamics of *Tyrannosaurus rex*. *Paleobiology*, *33*, 610–638.

Sookias, R. B., Butler, R. J., & Benson, R. B. J. (2012). Rise of dinosaurs reveals major body-size transitions are driven by passive processes of trait evolution. *Proceedings of the Royal Society B-Biological Sciences*, *279*, 2180–2187.

Stocker, M. R., Nesbitt, S. J., Criswell, K. E., Parker, W. G., Witmer, L. M., Rowe, T. B., Ridgely, R., & Brown, M. A. (2016). A dome-headed stem archosaur exemplifies convergence among dinosaurs and their distant relatives. *Current Biology*, *26*, 2674–2680.

Stubbs, T. L., Pierce, S. E., Rayfield, E. J., & Anderson, P. S. (2013). Morphological and biomechanical disparity of crocodile-line archosaurs following the end-Triassic extinction. *Proceedings of the Royal Society B-Biological Sciences*, *280*, 20131940.

Therrien, F., Henderson, D. M., & Ruff, C. B. (2005). Bite me: Biomechanical models of theropod mandibles and implications for feeding behavior. In K. Carpenter (Ed.), *The carnivorous dinosaurs* (pp. 179–237). Indiana University Press.

Thomason, J. J. (1995). *Functional morphology in vertebrate morphology*. Cambridge University Press.

Tolchard, F., Smith, R. M. H., Arcucci, A., Mocke, H., & Choiniere, J. N. (2021). A new 'rauisuchian' archosaur from the Middle Triassic Omingonde Formation (Karoo Supergroup) of Namibia. *Journal of Systematic Palaeontology*, *19*, 595–631.

Trotteyn, M. J., Desojo, J. B., & Alcober, O. (2011). Nuevo material postcraneano de *Saurosuchus galilei* (Archosauria: Crurotarsi) del Triásico Superior del centro-oeste de Argentina. *Ameghiniana*, *48*, 13–27.

Turner, A. H., & Nesbitt, S. J. (2013). Body size evolution during the *Triassic archosauriform* radiation. In S. J. Nesbitt, J. B. Desojo, & R. B. Irmis (Eds.), *Anatomy, phylogeny and palaeobiology of early archosaurs and their kin* (pp. 573–597). Geological Society, Special Publications.

van Valkenburgh, B. (1996). Feeding behaviour in free-ranging, large African carnivores. *Journal of Mammalogy*, *77*, 240–254.

van Valkenburgh, B., Teaford, M. F., & Walker, A. (1990). Molar microwear and diet in large carnivores: Inferences concerning diet in the sabertooth cat, *Smilodon fatalis*. *Journal of the Zoological Society of London*, *222*, 319–340.

Walker, A. D. (1964). Triassic reptiles from the Elgin area: *Ornithosuchus* and the origin of carnosaurs. *Transactions of the Royal Society of London, Series B, Biological Sciences*, *248*, 53–134.

Walker, J. D., Geissman, J. W., Bowring, S., & Babcock, L. (2013). The geological society of America geologic time scale. *GSA Bulletin*, *125*(3–4), 259–272.

Wallach, A. D., Izhaki, I., Toms, J. D., Ripple, W. J., & Shanas, U. (2015). What is an apex predator? *Oikos*, *124*, 1453–1461.

Walmsley, C. W., Smits, P. D., Quayle, M. R., McCurry, M. R., Richards, H. S., Oldfield, C. C., Wroe, S., Clausen, P. D., & McHenry, C. R. (2013). Why the long face? The mechanics of mandibular symphysis proportions in crocodiles. *PLoS One*, *8*, e53873.

Weinbaum, J. C. (2011). The skull of *Postosuchus kirkpatricki* (Archosauria: Paracrocodyliformes) from the Upper Triassic of the United States. *PaleoBios*, *30*, 18–44.

Weinbaum, J. C. (2013). Postcranial skeleton of *Postosuchus kirkpatricki* (Archosauria: Paracrocodylomorpha), from the Upper Triassic of the United States. In S. J. Nesbitt, J. B. Desojo, & R. B. Irmis (Eds.), *Anatomy, phylogeny and palaeobiology of early archosaurs and their kin* (Vol. 379, pp. 525–553). London, Special Publications.

Whitney, M. R., LeBlanc, A. R. H., Reynolds, A. R., & Brink, K. S. (2020). Convergent dental adaptations in the serrations of hypercarnivorous synapsids and dinosaurs. *Biology Letters*, *16*, 20200750.

Wilkenros, C., Sand, H., Ahlqvist, P., & Liberg, O. (2013). Biomass flow and scavengers use of carcasses after re-colonization of an apex predator. *PLoS One*, *8*, e77373.

Winkler, D. E., Kubo, T., Kubo, M. O., Kaiser, T. M., & Tütken, T. (2022). First application of dental microwear texture analysis to infer theropod feeding ecology. *Palaeontology*, *65*, e12632.

Young, C. C. (1973). On the occurrence of *Vjushkovia* in Sinkiang. *Memoirs of the Institute of Vertebrate Paleontology and Paleoanthropology*, *10*, 38–52.

Zapata, U., Metzger, K. A., Wang, Q., Elsey, R. M., Ross, C. F., & Dechow, P. C. (2010). Material properties of mandibular cortical bone in the American alligator, *Alligator mississipiensis*. *Bone*, *46*, 860–867.

SUPPORTING INFORMATION

Additional supporting information can be found online in the Supporting Information section at the end of this article.

How to cite this article: Fawcett, M. J., Lautenschlager, S., Bestwick, J., & Butler, R. J. (2023). Functional morphology of the Triassic apex predator *Saurosuchus galilei* (Pseudosuchia: Loricata) and convergence with a post-Triassic theropod dinosaur. *The Anatomical Record*, 1–17. https://doi.org/10.1002/ar.25299